Chapter 1

Lattice Structure, Phonons, and Electrons

1.1 Introduction

Guessing the technical background of students in a course or readers of a book is always a hazardous enterprise for an instructor, yet one must start a book or a course *somewhere* on the landscape of knowledge. Here, we begin with some essential concepts from condensed-matter physics and statistical mechanics. The definition of essential, too, is questionable and is presently intended to be information that recurs too frequently in the later parts of the text to leave the requisite information to the many excellent reference sources on these subjects.

Our overarching objective is to develop the tools required to predict thermal transport in structures such as the one shown in Fig. 1.1. Arguably the most important thermal characteristic of an object is its thermal conductivity (κ) defined as:

$$\kappa \equiv \frac{[\text{rate of heat flow (in W)}] \times [\text{object length (in m)}]}{[\text{cross-sectional area (in m}^2\text{)}] \times [\text{temperature drop (in K)}]}. \quad (1.1)$$

For roughly a century, thermal conductivity was considered a basic material property in the engineering sense (e.g., with minor accommodation for variations in temperature), and therefore, the effects of the geometric terms in Eq. (1.1) were assumed to normalize with the others such that the final property was independent of size and shape. However, with the advent of microscale fabrication (and later nanoscale fabrication), the technical community was able to create tiny materials that exhibited deviations from the size-independent property assumption. In such circumstances, knowledge of not only a material's size and shape becomes crucial but also the details of the atomic-scale carriers of thermal energy (Chen, 2005). At this

level, in order to retain the utility of the concept of thermal conductivity (and it does remain useful for many purposes) we need to understand many additional factors, including:

- What type of quantum-mechanical carrier dominates heat flow in the material?
- How is thermal energy distributed among these carriers?
- How fast do the carriers move through the material?
- How much thermal energy does each carrier hold as it moves?
- How do the carriers scatter as they move through the material?
- How do the boundaries and interfaces impede carriers?

The answers to these questions require a much deeper perspective on the mechanisms of thermal energy transport than is provided in traditional engineering expositions on heat conduction. Thus we embark here on the first of two background chapters: the present on lattice structure and the subsequent on statistics of energy carriers.

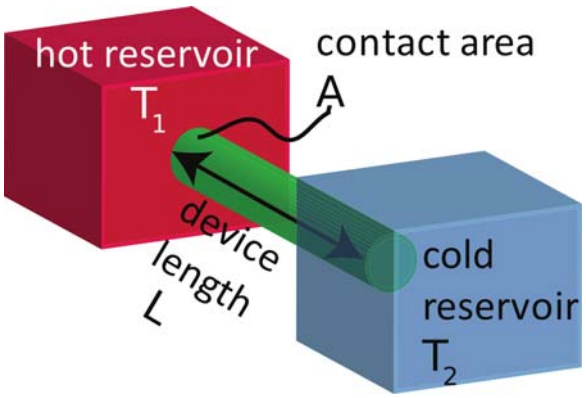

Fig. 1.1 Schematic of a general contact-device-contact arrangement.

The study of thermal energy in any material should rightly begin with a description of the material itself, for thermal energy, unlike other forms of energy such as optical, electronic, and magnetic, is routinely generated, stored, and transported by a diverse set of 'carriers'. The reason for broader context of thermal energy derives from the second law of thermodynamics, which dictates that all forms of energy tend toward disorder (or 'thermalization'). In this text, we will make every reasonable attempt to unify the

analysis, i.e., to generalize concepts so that they apply to multiple carriers, but this objective is occasionally elusive. In such cases, the text will make clear the relevant restrictions by carrier and material types. The list of interesting materials and physical structures is almost endless, and therefore given the subject of 'nanoscale' physics, the text begins with an admittedly cursory treatment of interatomic bonding but then highlights where possible a compelling structure — the graphene carbon lattice — to illustrate important and unique thermal behavior at the nanoscale.

1.2 Atom-to-Atom Bonding in Solid Lattices

The details of interatomic bonding determine a broad assortment of physical material properties, ranging from mechanical strength to electrical conductivity. The primary interest here relates to the resultant vibrational characteristics of atoms that exist in an ordered arrangement, i.e., in a regular crystal. However, we start with a simpler situation: that of a diatomic molecule.

Figure 1.2 shows a schematic of two atoms separated by an equilibrium distance $r = r_0$ about which the atoms vibrate at various (but restricted) frequencies. A generic potential energy field $U(r)$ between the atoms is shown in the bottom half of the figure, revealing the strong repulsive force ($F = -\partial U/\partial r$) when the atoms are close together ($r < r_0$). The minimum energy (at $r = r_0$) corresponds to the bond energy, as the potential energy asymptotes to zero when the atoms are pulled apart ($r \to \infty$).

The mathematical form of the potential can be very complicated and is itself the subject of intensive research through both first-principles (*ab initio*) approaches such as density functional theory (Saha *et al.*, 2008) and empirically derived potentials (Tersoff, 1988). For the time being, we consider a simplification of the potential, focusing on the near-minimum region where the potential is typically well approximated by a parabolic relation with respect to the equilibrium displacement $u = r - r_0$ such that $U \sim u^2$. The constant of proportionality plays an important role in the dynamics of molecules and lattices, for it contains the *effective spring constant* g of the bond:

$$U = \frac{1}{2} g u^2. \tag{1.2}$$

This so-called harmonic approximation is depicted in Fig. 1.3. We note that lattice vibrations typically involve small displacements; therefore, the

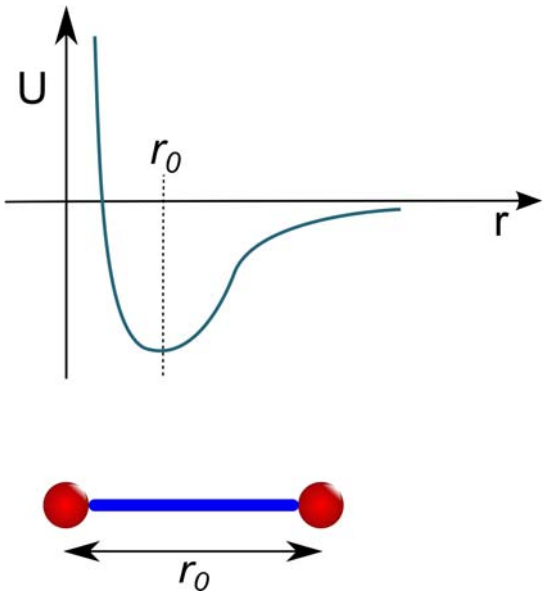

Fig. 1.2 Variation of potential energy field $U(r)$ with interatomic distance r. $r = r_0$ corresponds to the equilibrium separation with minimum potential energy.

harmonic approximation tends to predict the overall vibrational states (or what we will call the *vibrational eigenspectrum*) with good accuracy. The deviations, or anharmonicities, however, play an important role in phonon scattering, as discussed in Chapter 5.

One issue that we will cover only briefly is how such bonds form. Referring to Fig. 1.4, when two self-contained atoms [Fig. 1.4(a)] are brought together [Fig. 1.4(b)], their electrons can interact and begin to share orbitals. However, the energies of the orbitals must change because of restrictions imposed by the Pauli exclusion principle on the quantum states of electrons; therefore, upon bonding, the energy levels depicted by horizontal lines in Fig. 1.4, undergo small shifts.

These electronic interactions define the nature and strength of interatomic bonds and can produce many different bond types and energies (E_b), including:

- van der Waals: weak bond due to dipole moments, $E_b \sim 0.01$ eV
- Hydrogen: due to electronegative atoms (e.g., O in H_2O), $E_b \sim 0.1$ eV

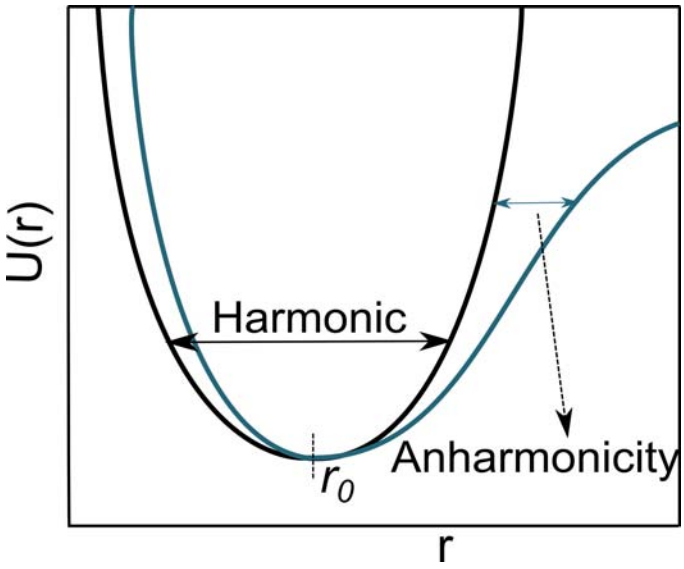

Fig. 1.3 Harmonic approximation to the real interatomic potential with anharmonicity. At small displacements, the harmonic potential is a good approximation.

- Covalent: atoms share valence electrons (e.g., Si and diamond), $E_b = 1 \sim 10$ eV
- Ionic: one atom gives up its electron, forms ions with Coulombic binding forces, $E_b = 1 \sim 10$ eV
- Metallic: like covalent bonds, but with freely moving electrons, $E_b = 1 \sim 10$ eV

We will focus on thermal energy in solid materials, but some of the content such as kinetic theory in Chapter 3 applies equally well to fluid phases. Within the array of solid-state materials, single-crystal structures are the most amenable for initial study, although even these structures become rather complex in three dimensions with various atomic arrangements such as face-centered cubic (fcc), body-centered cubic (bcc), and diamond configurations that are perhaps most familiar to readers. To minimize digression, here we refer the reader to the many excellent textbooks on solid-state physics (Ashcroft and Mermin, 1976; Kittel, 2007) and crystallography (De Graef and McHenry, 2012) for advanced treatment of 3D crystals.

We will focus on one- and two-dimensional lattices for the sake of expediency and because the 2D graphene lattice has high contemporary

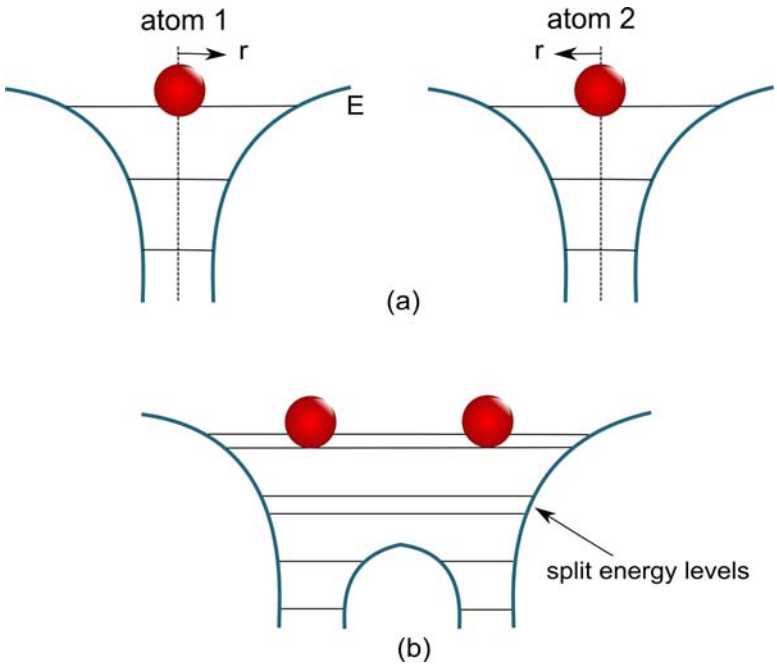

Fig. 1.4 (a) Two isolated, self-contained atoms and associated electron energy states. (b) Quantized energy states upon bond formation between the two isolated atoms. Energy levels are modified as electron orbitals become shared in a bond.

scientific and technological importance. A simple 1D structure is obtained by repeating the diatomic arrangement of Fig. 1.2 indefinitely. Figure 1.5 shows the resulting configuration, with each atom of mass m connected to its neighbor by a bond with spring constant g. The equilibrium separation between atoms is represented by the lattice constant a. Somewhat surprisingly, this simple, idealized structure will enable us to develop almost all the essential tools for analysis of lattice vibrations and their quantum manifestation—called phonons.

Because an ideal crystal extends infinitely in all directions, we must find a way to concentrate the analysis on a smaller region. Fortunately, the regular order, or periodicity, of a crystal lattice makes this task straightforward. A *primitive unit cell* of a lattice is one that, if repeated throughout all space by well-defined translational vectors, would fill the space entirely and with no overlapping regions or void spaces. Figure 1.6 shows an example for a 2D monatomic rectangular lattice. Several possible shapes, positions, and

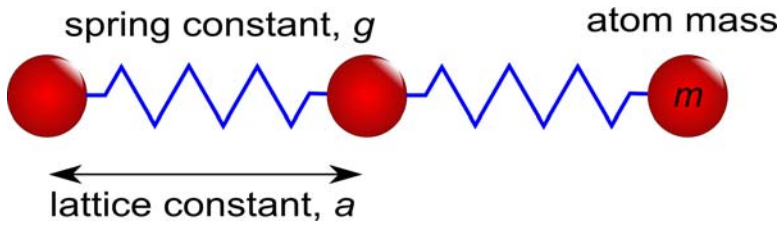

Fig. 1.5 An ideal 1D crystal modeled as periodic atom-spring-atom system.

orientations of the primitive unit cell exist for this lattice, as indicated by the shaded regions. The arrows denote *basis vectors* ($\vec{a}_i$) that define the periodic translation of the unit cells throughout the domain. The set of all possible translations by integer indexing of basis vectors forms a so-called Bravais lattice, whose discrete points are given by the lattice vector $\vec{R}$:

$$\vec{R} = \sum_i n_i \vec{a}_i \overset{\text{in 2D}}{=} n_1 \vec{a}_1 + n_2 \vec{a}_2. \tag{1.3}$$

For the linear 1D chain, the sole lattice vector is simply the lattice constant a.

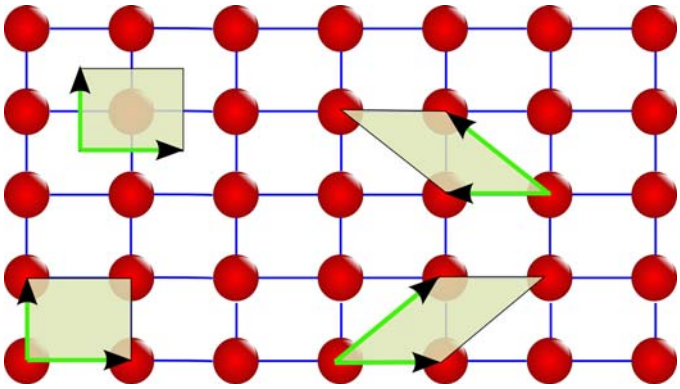

Fig. 1.6 An ideal 2D monatomic rectangular lattice represented by periodic translation of valid primitive cells (shaded green) defined by green basis vectors.

As might be expected given the complexity of our natural world, a Bravais lattice alone cannot describe the atomic positions of all real crystals. For such cases, we resort to defining the positions of multiple atoms

(usually two) at each nodal site in the Bravais lattice. This approach is quite understandable for compounds such as crystalline SiO_2 (quartz), but it is also necessary to describe the lattice geometry of some monatomic crystals, including technologically important ones such as silicon and diamond. Figure 1.7 shows the crystal construction in 2D, with the multi-atom basis pair placed regularly on spatially distributed Bravais lattice points.

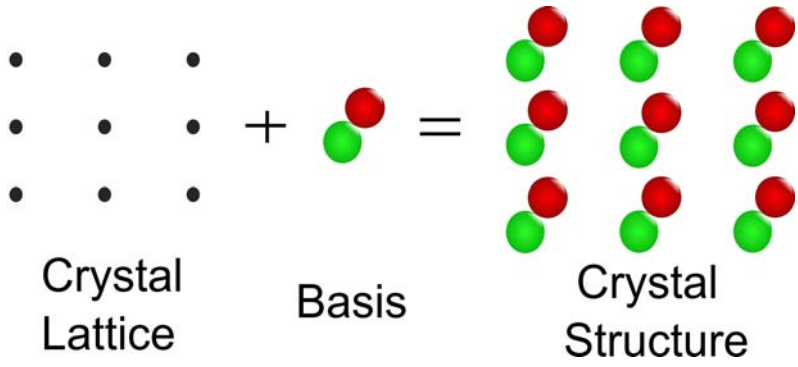

Fig. 1.7 Structure of a two-atom basis crystal. Each nodal site of the lattice contains a two-atom basis that defines the complete crystal structure upon translation through all possible lattice vectors.

One of the most fascinating 2D lattices, and one of intense contemporary study, is graphene, which consists entirely of carbon atoms in hexagonal arrangement on a 2D plane as shown in Fig. 1.8. The equilibrium distance between nearest carbon atoms is $\tilde{a} = 1.42$ Å, where the '˜' denotes a bond length (often the lattice constant and bond lengths differ for more complex lattices). Different edge configurations are possible in graphene, and the two most common are shown in the figure. Importantly, graphene is one of the monatomic structures that requires the addition of a basis atom to describe the full lattice. Its basis vectors, as shown in Fig. 1.9, are:

$$\begin{aligned} \vec{a}_1 &= \frac{3}{2}\tilde{a}\hat{x} + \frac{\sqrt{3}}{2}\tilde{a}\hat{y} \\ \vec{a}_2 &= \frac{3}{2}\tilde{a}\hat{x} - \frac{\sqrt{3}}{2}\tilde{a}\hat{y}. \end{aligned} \tag{1.4}$$

The vector that connects the primary and basis atoms within a unit cell is simply $\vec{a}_b = \tilde{a}\hat{x}$.

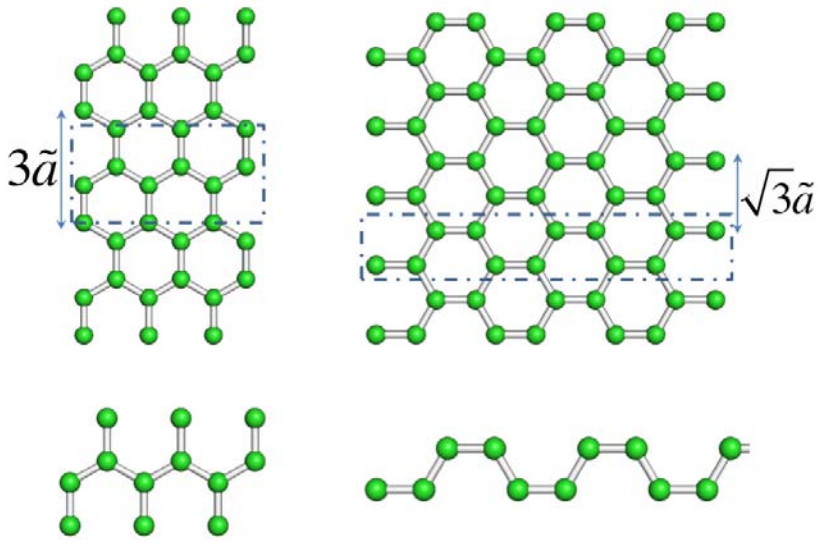

Fig. 1.8 Graphene nanoribbon crystal structure. The left structure is the armchair configuration; the right structure is zigzag. Dashed rectangles represent a graphene nanoribbon unit cell. The unit cell for each configuration is displayed below the crystal lattice structure.

1.3 Mathematical Description of the Lattice

The analysis of crystals can seem challenging in comparison to that of individual molecules because of the former's vast size. To overcome this challenge, we take advantage of a crystal lattice's *translational symmetry*. This approach requires a mathematical description that inverts space such that large entities become small.

We describe something large in terms of small things in the common way–with Fourier transforms. We start again with 1D chain of atoms and allow for the possibility that these atoms have a distributed mass density ρ. Perfect periodicity with lattice constant a (see Fig. 1.10) implies that:

$$\rho(x + ma) = \rho(x), \tag{1.5}$$

where m is any integer.

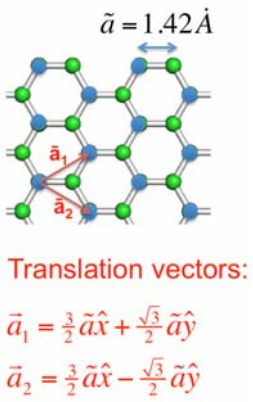

Fig. 1.9 Basis vectors for the graphene crystal structure.

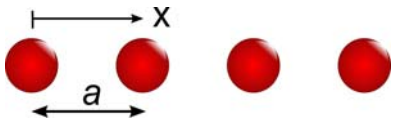

Fig. 1.10 Perfect periodic 1D chain of atoms with lattice constant a.

Each density function $\rho(x)$ and $\rho(x+ma)$ can be expanded in a Fourier series such that Eq. (1.5) becomes:

$$\begin{aligned} \rho(x) &= \sum_n \rho_n \exp\{iG_n x\} \\ = \rho(x+ma) &= \sum_n \rho_n \exp\{iG_n(x+ma)\} \\ &= \sum_n \rho_n \exp\{iG_n x\} \exp\{iG_n ma\}, \qquad (1.6) \\ \rightarrow \exp\{iG_n ma\} &= 1 \rightarrow G_n ma = 2\pi \times \text{integer}, \qquad (1.7) \end{aligned}$$

where n and m are indexing integers. The last relation, Eq. (1.7), severely restricts the possible values of G. This restriction should not be surprising because the original density function, ρ, is strictly periodic and in the limit of point masses represents a series of delta functions. In fact, the series of real-space lattice points at $a, 2a, 3a, \ldots$ for this simple 1D problem is simply the Bravais lattice vector defined by $\vec{R} = na\hat{x}$.

Extending to multiple dimensions, the restrictive relation between $\vec{G}$ and $\vec{R}$ is:

$$\vec{G}_n \cdot \vec{R}_m = 2\pi \times \text{integer}. \tag{1.8}$$

The vector $\vec{G}$ thus becomes critically important in the description of lattices–*the reciprocal lattice vector*. In the interest of brevity and following the lead of Ziman, we will not be "concerned here with mathematically pathological functions, and may use naive Fourier theory quite freely" (Ziman, 1972). As such, we will simply state the relations between reciprocal lattice translation vectors $\vec{b}_i$ and the direct lattice translation vectors $\vec{a}_i$ in 3D:

$$\vec{G} = k_1\vec{b}_1 + k_2\vec{b}_2 + k_3\vec{b}_3, \tag{1.9}$$

where

$$\vec{b}_i = 2\pi \frac{\vec{a}_j \times \vec{a}_k}{\vec{a}_1 \cdot (\vec{a}_2 \times \vec{a}_3)}, \tag{1.10}$$

and k_i are integers, and the denominator in Eq. (1.10) is the unit cell volume.

Once the $\vec{b}_i$ vectors are known, the reciprocal space can be populated with discrete points. We will focus on 2D graphene here. Analysis of the primitive translational vectors in Eq. (1.4) in the context of Eq. (1.8) reveals that we must have $\vec{b}_1 \perp \vec{a}_2$ and $\vec{b}_2 \perp \vec{a}_1$ and that

$$\begin{aligned} \vec{b}_1 &= C_1 \left[\frac{\sqrt{3}}{2}\hat{x} + \frac{3}{2}\hat{y} \right] \\ \vec{b}_2 &= C_2 \left[\frac{\sqrt{3}}{2}\hat{x} - \frac{3}{2}\hat{y} \right]. \end{aligned} \tag{1.11}$$

The constants C_1 and C_2 must be equal to preserve the generality of Eq. (1.8), and given the magnitude of the vectors $|\vec{a}_i| = \sqrt{3}\tilde{a}$, we find:

$$\begin{aligned} C_1 = C_2 &= \frac{4\pi}{a3\sqrt{3}} \\ \rightarrow \vec{b}_1 &= \frac{2\pi}{\tilde{a}} \left[\frac{1}{3}\hat{x} + \frac{1}{\sqrt{3}}\hat{y} \right] \\ \rightarrow \vec{b}_2 &= \frac{2\pi}{\tilde{a}} \left[\frac{1}{3}\hat{x} - \tfrac{1}{\sqrt{3}}\hat{y} \right]. \end{aligned} \tag{1.12}$$

The resulting lattices, both direct (a) and reciprocal (b), for graphene are shown in Fig. 1.11, as well as the respective translational vectors and the so-called 1st Brillouin zone, which is hexagonal in shape. The reciprocal lattice's primitive cell (i.e., 1st Brillouin zone) is established by connecting lattice points with lines, which then define the shaded region of 2D space closest to a given lattice point.

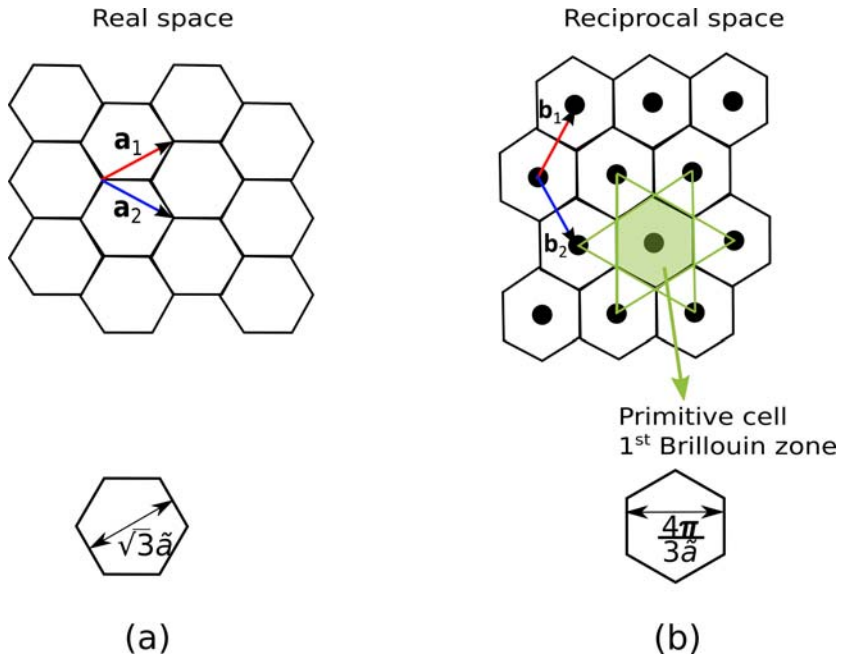

Fig. 1.11 (a) Direct graphene lattice. (b) Reciprocal graphene lattice. The primitive cell of the reciprocal lattice is the 1st Brillouin zone. Translation vectors of both lattices are also depicted.

Reciprocal space is often termed '**k**-space', and we will use the terms interchangeably. Reciprocal space is also useful in defining directions in a crystal. For a given real-space lattice plane, the Miller indices $(k_1k_2k_3)$ are vector coordinates (see Eq. (1.12)) of the shortest reciprocal lattice vector normal to the plane. The Miller indices should not be confused with the primary directions in the real-space lattice, which are denoted by square brackets $[xyz]$.

1.4 Lattice Vibrations and Phonons

The description of lattice vibrations starts with the potential-energy/displacement relation of Eq. (1.2). When constructed as a linear chain of atoms, the individual potential energies from each compressed or expanded spring are summed to form the harmonic potential energy U^{harm}:

$$U^{\text{harm}} = \frac{1}{2} g \sum_n \{u[na] - u[(n+1)a]\}^2, \tag{1.13}$$

where the terms na and $(n+1)a$ designate the spatial positions of the atoms. The force on an individual atom (at, say, location na) can be calculated from the spatial derivative of displacement at that location:

$$F = m\frac{d^2u(na)}{dt^2} = -\frac{\partial U^{\text{harm}}}{\partial u(na)} = -g\left\{2u(na) - u\left[(n-1)a\right] - u\left[(n+1)a\right]\right\}, \tag{1.14}$$

where the factor 2 appearing in $2u(na)$ is the result of the fact that location 'na' appears twice in the summation of Eq. (1.13) (once as $(n+1)a$ and then as na as the sum proceeds). The 'na' nomenclature becomes quite tedious in practice, and we therefore simplify the expression of Eq. (1.14) as:

$$m\frac{d^2u_n}{dt^2} = -g\left\{2u_n - u_{n-1} - u_{n+1}\right\}. \tag{1.15}$$

The solution of Eq. (1.15) requires boundary conditions, and the simplest are the so-called Born-von Karman type in which the ends of the 1D chain are attached as in a loop (see Fig. 1.12). We note that this 'loop' does not add a new dimension to the problem, as the number of atoms N is assumed to be very large.

The Born-von Karman boundary conditions become:

$$\begin{aligned} u_N &= u_0 \\ u_{N+1} &= u_1. \end{aligned} \tag{1.16}$$

We assume a plane-wave solution for displacement at location n as:

$$u_n(t) \sim \exp\left\{i\left(Kna - \omega t\right)\right\}, \tag{1.17}$$

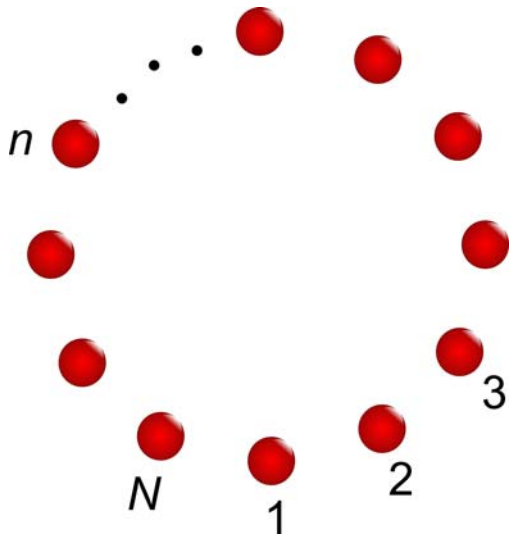

Fig. 1.12 1D chain of N atoms with the Born-von Karman boundary condition.

where K is the wavevector of the plane wave and is proportional to the inverse of wavelength. Application of Eq. (1.17) to the boundary conditions above yields:

$$\begin{aligned} u_{N+1} &\sim \exp\{i\left[K\left(N+1\right)a - \omega t\right]\} \\ u_1 &\sim \exp\{i\left[Ka - \omega t\right]\} \\ \rightarrow 1 &= \exp\left[iKNa\right] \rightarrow KNa = 2\pi n, \end{aligned} \tag{1.18}$$

where n is an indexing integer. The final relation in Eq. (1.18) is of crucial importance, for it restricts the possible values of the wavevector K that can 'fit' on the looped 1D chain. Of course, if the number of total atoms N is large, then many wavevectors are possible. Defining the wavelength as $\lambda_n = aN/n$, the set of allowed wavevectors becomes:

$$K_n = \frac{2\pi n}{aN} = \frac{2\pi}{\lambda_n}. \tag{1.19}$$

Finally, we note that the minimum size of a wave (wavelength) is $\lambda_{\min} = 2a$, for any shorter waves would not have atoms to sustain them. Another way of explaining this characteristic is that any smaller wavelengths would have nodal positions (in the standing wave sense) that could

be described by longer waves in which the nodal positions would exist on lattice sites, instead of between atoms. Consequently, the maximum unique wavevector is:

$$|K_{\max,\text{unique}}| = \frac{\pi}{a}. \tag{1.20}$$

This important restriction enables us to convert what is an infinite domain in real space (as $N \to \infty$) into a finite domain in reciprocal space ($K \in [-\pi/a, \pi/a]$), with the associated advantages of mathematical convenience. Importantly, this unique region of reciprocal space (or **k**-space) coincides with the 1st Brillouin zone.

We now return to the equation of motion, Eq. (1.15), and its solution. Substitution of the plane-wave function of Eq. (1.17) for position na and incorporation of the discrete wavevectors K_j produces:

$$\begin{aligned} -m\omega_j^2 e^{i(K_i na-\omega_j t)} &= -g\left[2 - e^{-iK_j a} - e^{iK_j a}\right] e^{i(K_j na-\omega_j t)} \\ &= -2g\left(1-\cos K_j a\right) e^{i(K_j na-\omega_j t)}. \end{aligned} \tag{1.21}$$

The resulting relationship between frequency and wavevector defines the *dispersion relation* of the lattice:

$$\omega_j(K_j) = \sqrt{\frac{2g(1-\cos K_j a)}{m}} = 2\sqrt{\frac{g}{m}}\left|\sin(\tfrac{1}{2}K_j a)\right|. \tag{1.22}$$

The continuous form of this relation ($\omega(K)$, which we will use hereafter, dropping the subscript j) is sketched in Fig. 1.13. We note that the maximum frequency depends quite simply on the spring constant and atomic mass, as $\omega_{\max} = 2\sqrt{g/m}$.

The dispersion relation contains information pertinent to a wide range of material characteristics, from elastic constants to the scattering rates of phonons. We will discuss many of these in context throughout the remainder of the text. For now, we highlight the phase and group velocities:

$$\textit{phase velocity:}\ \ c = \frac{\omega}{K}, \tag{1.23}$$

$$\textit{group velocity:}\ \ v_g = \frac{\partial\omega}{\partial K}. \tag{1.24}$$

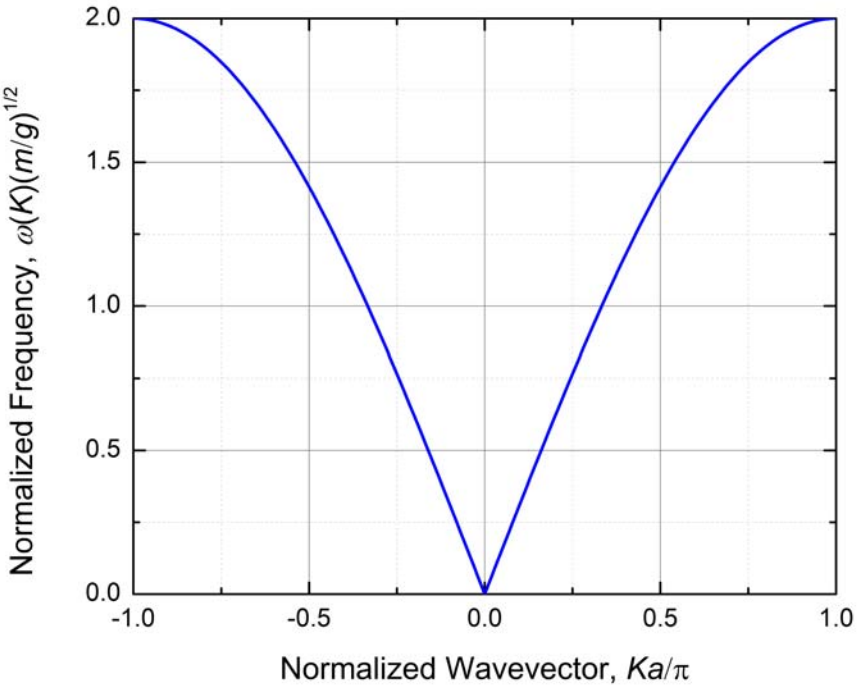

Fig. 1.13 Dispersion relation for a monatomic 1D chain of atoms.

Most of our interest will be given to the group velocity because it determines the rate of energy transport. Further, we will often focus on the long-wave limit ($K \to 0$), for which:

$$\lim_{K\to 0} \omega = a\sqrt{\frac{g}{m}}\,|K|$$

$$\to \lim_{K\to 0} v_g = a\sqrt{\frac{g}{m}} = \left|\frac{\omega}{K}\right| = c. \tag{1.25}$$

In this limit, the group and phase velocities are equal, and they both are the same as the speed of sound in the solid. Therefore, the types of phonons that exhibit this behavior (other types are considered later) are termed *acoustic phonons*.

Thus far we have used strictly classical descriptions of mechanical vibrations to derive the vibrational spectrum of the lattice. However, to treat collections of vibrations (because a lattice can support many vibrational

modes at the same time), we must transition to a quantum description. Nevertheless, we can retain the results from the classical harmonic oscillator solution above to define each *normal mode* in terms of a wavevector K and frequency ω (i.e., the dispersion relation remains valid). A solution of the time-independent Schrödinger equation of quantum mechanics (see Eq. (1.31) in the next section) reveals that each mode can contain a set of energies described by:

$$\varepsilon_K = \left(N_K + \tfrac{1}{2}\right)\hbar\omega_K, \tag{1.26}$$

where N_K represents the number of phonons with wavevector K, and the terminology ω_K is intended to signify the inherent relationship between frequency and wavevector embodied by the dispersion relation (Eq. (1.22)). The $\frac{1}{2}$ term in Eq. (1.26) accounts for the so-called zero-point energy whose derivation is available elsewhere (Ashcroft and Mermin, 1976, Appendix L). The term N_K defines the average number of such excited modes of wavevector K, or the number of *phonons*, and is defined by Bose-Einstein statistics:

$$N_K = \frac{1}{\exp\left(\frac{\hbar\omega_K}{k_B T}\right) - 1}, \tag{1.27}$$

where k_B is Boltzmann's constant, and T is temperature. We will later use the symbol f^o_{BE} as a synonym for N_K (in attempt to maintain some consistency while also identifying various symbols that are used in the literature for the occupation number).

The connection between the quantum energy of Eq. (1.26) and the classical vibration amplitude is often elusive to new learners and is therefore included here to connect with mechanical intuition. Classically, each vibrational mode contains a combination of potential and kinetic energy that can be shown to be, on average, equal in magnitude by the virial theorem (Ashcroft and Mermin, 1976) such that:

$$\bar{\varepsilon}_{\text{classical}} = \sum_{\text{lattice}} m\left|\dot{u}\right|^2, \tag{1.28}$$

where the"$\dot{}$" denotes time differentiation. For a simple lattice of N atoms with one atom of mass m per unit cell, the summation can be transformed

to reciprocal space as:

$$\bar{\varepsilon}_{\text{classical}} = \sum_K N m \omega_K^2 \left|\tilde{u}_K\right|^2, \tag{1.29}$$

where $|\tilde{u}_K|$ is the amplitude of atomic displacement for a mode with wavevector K. Equating the summed term in Eq. (1.29) with the quantum version (Eq. (1.26)), the relationship between displacement amplitude and (quantized) energy becomes:

$$\begin{aligned} \left|\tilde{u}_K\right|^2 &= \frac{\varepsilon_K}{N m \omega_K^2} \\ &= \frac{\left(N_K + \frac{1}{2}\right)\hbar}{N m \omega_K}. \end{aligned} \tag{1.30}$$

This result should be intuitive, for it indicates that displacement amplitude increases with increasing occupation number and decreases with increasing frequency, both in the square-root sense. An illustration of phonon quantization, showing the relationship between allowed energies and atomic displacements, is shown in Fig. 1.14. For further details, the reader is referred to Ziman (1972).

Still remaining in our development is the extension of the foregoing principles of dispersion and energy to multiple dimensions and orientations of oscillations relative to the propagation direction (i.e., polarization). We defer these subjects to later chapters, when they can be developed in better context.

1.5 Free Electrons

Electronic behavior varies widely among different types of materials, from 'free' conduction in metals to virtually none in insulators. In this chapter we will consider only metals, and even then we will use the simplest approximation–free electron theory. Later chapters elucidate more complicated electronic structure.

The fundamental equation governing quantum particles is Schrödinger's equation, whose time-independent form is:

$$\frac{-\hbar^2}{2m_e}\nabla^2\Psi(\vec{r}) + \mathcal{V}(\vec{r})\Psi = E\Psi(\vec{r}), \tag{1.31}$$

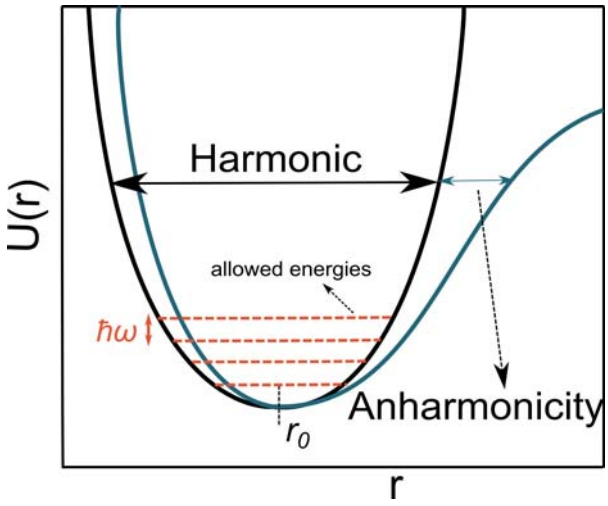

Fig. 1.14 Discrete energy levels depict phonon quantization. Successive energy levels are separated by $\hbar\omega$.

where Ψ is the electron wavefunction, and $\mathcal{V}(\vec{r})$ represents a potential energy function that commonly represents the periodic ion field in a crystal. However, $\mathcal{V}(\vec{r}) = 0$ is assumed to make electrons 'free' in the present simplification. The wavefunction determines the probability per unit volume P of finding an electron at position $\vec{r}$ according to:

$$P = \left|\Psi(\vec{r})^2\right| = \Psi(\vec{r})\Psi^*(\vec{r}), \tag{1.32}$$

where the "*" denotes complex conjugation. Once again, we assume a plane-wave solution (in this case, a steady-state form):

$$\Psi_k(\vec{r}) = \frac{1}{\sqrt{V}} e^{i\vec{k}\cdot\vec{r}}, \tag{1.33}$$

where V is volume and $\vec{k}$ is the electron's wavevector.[1] Substitution into the governing equation yields an expression for the energy eigenvalue E_k:

$$E_k = \frac{\hbar^2 k^2}{2m_e}, \tag{1.34}$$

[1] We will use the lowercase symbol k for electrons, and the uppercase K for phonons to signify the carrier type. The term **k**-space is generic and applies to either.

where $k = \left|\vec{k}\right|$. Equation (1.34) relates electron energy and wavevector and is the dispersion relation for electrons, analogous to Eq. (1.22) for phonons. In this case, the functional relationship is parabolic, $E_k \sim k^2$. Such parabolic dispersion relations (or bands) are common in real materials, even for those with complicated electronic structures.

The parabolic '$E-k$' relation suggests a connection between wavevector and momentum. The usual Newtonian expressions for momentum p and energy become:

$$\begin{aligned} &|p| = m_e\,|v|\,;\ E = \frac{m_e v^2}{2} \rightarrow v = \sqrt{\frac{2E}{m_e}} \\ &\rightarrow |p| = m_e\sqrt{\frac{2E}{m_e}} = \sqrt{2Em_e} = \sqrt{\hbar^2 k^2} = \hbar k \\ &\rightarrow \vec{p} = \hbar\vec{k}. \end{aligned} \tag{1.35}$$

The final result indicates that the wavevector can be considered a surrogate for momentum.

The momentum of electrons is restricted to certain allowed states, as it was for phonons. For the free electron gas, we can determine these values by considering an electron in a cube (the so-called 'electron in a box' problem). The wavefunction and its corresponding probability functional in Eq. (1.32) are assumed to be spatially periodic (see Fig. 1.15), such that:

$$\Psi(x+L) = \Psi(x);\ \Psi(y+L) = \Psi(y);\ \Psi(z+L) = \Psi(z). \tag{1.36}$$

Combining these periodic conditions with the plane-wave solution of Eq. 1.33 produces a set of allowable wavevectors:

$$\begin{aligned} &e^{ik_x L} = e^{ik_y L} = e^{ik_z L} = 1 \\ &\rightarrow k_x = \frac{2\pi n_x}{L}, k_y = \frac{2\pi n_y}{L}, k_z = \frac{2\pi n_z}{L}, n_i = 1, 2, 3, \ldots \end{aligned}. \tag{1.37}$$

This result should be familiar, for it is the same as that for phonons in the linear chain (Eq. (1.19)) for $L = aN$, the chain length. Therefore, allowable wavevectors are separated by $2\pi/L$ in reciprocal space; this characteristic will be useful in the next chapter in deriving the so-called density of states.

An important difference exists, however, between the manner in which the allowed wavevectors are populated for electrons and phonons. The latter can populate a state with a limitless number whose average (which need

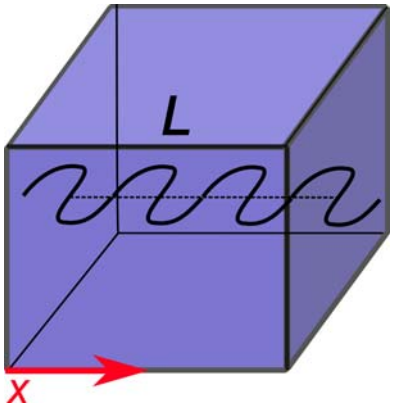

Fig. 1.15 Electron in a cube with a spatially periodic wavefunction.

not be an integer) is given by Eq. (1.27). Conversely, the electron occupation number of a given state is limited by the Pauli exclusion principle to be either 0 (not occupied) or 1 (occupied). Therefore, free electrons readily fill the reciprocal space until the number of carriers is exhausted.

Consider a material that contains N' free electrons in a volume of real space V. The ratio of these is the electron density $\eta_e = N'/V$. Because each allowed state occupies a reciprocal-space volume of $(2\pi/L)^3$, the number of electrons can be expressed in terms of a spherical 'volume' of **k**-space as:

$$N' = 2\frac{\left(4\pi k^3/3\right)}{\left(2\pi/L\right)^3} = \frac{k_F^3}{3\pi^2}V, \tag{1.38}$$

where k_F is called the Fermi wavevector and represents the largest occupied state at absolute zero temperature (the next chapter considers non-zero temperatures). The factor 2 in Eq. (1.38) accounts for the two electron spin states–up and down.

Other Fermi quantities can be easily derived from the Fermi wavevector:

$$\text{Fermi wavevector: } k_F = \left(3\pi^2\eta_e\right)^{1/3}, \tag{1.39}$$

$$\text{Fermi energy: } E_F = \frac{\hbar^2 k_F^2}{2m_e} = \frac{\hbar^2}{2m_e}\left(3\pi^2\eta_e\right)^{2/3}, \tag{1.40}$$

$$\text{Fermi velocity: } v_F = \frac{\hbar k_F}{m_e} = \frac{\hbar}{m_e}\left(3\pi^2\eta_e\right)^{1/3}, \tag{1.41}$$

$$\text{Fermi temperature: } \theta_F = \frac{E_F}{k_B} = \frac{\hbar^2}{2m_e k_B}\left(3\pi^2\eta_e\right)^{2/3}. \tag{1.42}$$

The Fermi energy E_F is the most commonly used, and as shown in Eq. (1.40), can be calculated from the electron density. The Fermi velocity v_F is also an important quantity because even though the electron velocities cover a very broad range, only states near the Fermi level are active in conduction because of the nearby availability of unoccupied states necessary to produce transport.

A sketch of the filled and empty energy levels is shown in Fig. 1.16. By convention, the zero energy datum is chosen to sit at the bottom of the conduction band, with non-conducting core electron states beneath. The electrons fill energies upward until they reach the Fermi energy and are contained in the solid by an energy barrier called the work function ϕ, which is the difference between the vacuum energy E_{vac} and Fermi energy E_F.

1.6 Example: 1D Atomic Chain with a Diatomic Basis

We choose a diatomic 1D chain of atoms as shown schematically in Fig. 1.17 to demonstrate a slightly more complicated situation than the monatomic chain of Section 1.4. The 2-atom basis produces an entirely separate phonon branch, as derived below.

For details of phonon analysis for linear chains, the reader is referred to Chapter 2 of Ziman (1972). We note that the definition of a here, which is the distance between unit cells, is a bit different from Ziman's, which does not span a full unit cell but rather the distance between atoms within a cell. Here we include the essential elements starting again with the Lagrangian mechanics relation, $\mathbf{F} = m\ddot{\mathbf{u}} = -\nabla U^{\text{harm}}$ (cf., Eq. (1.14)), where $\mathbf{F}$ is the force on a particle of mass m with displacement $\mathbf{u}$, and again U^{harm} is the potential energy of the entire many-body system. Given the one-dimensional nature of the present formulation, we drop the spatial vector notation.

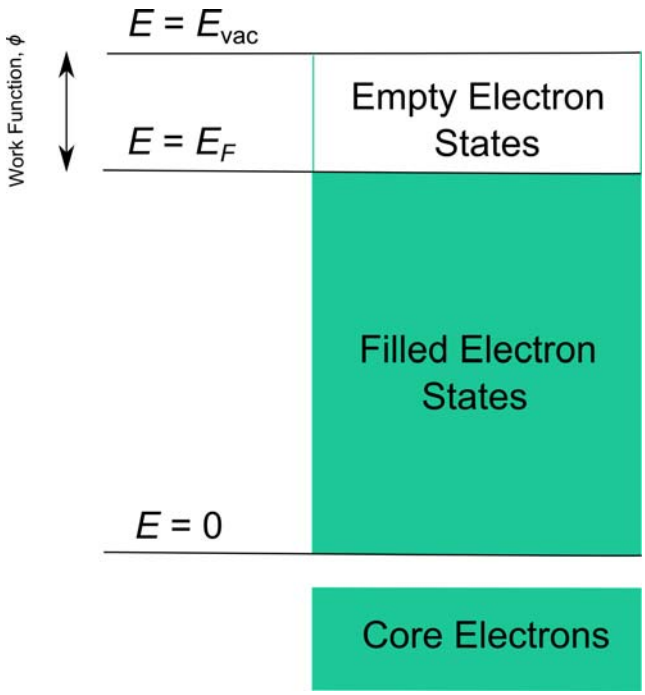

Fig. 1.16 Sketch of filled and empty electron energy states. The work function, ϕ, is defined as the difference between the Fermi energy, E_F, and the vacuum energy, E_{vac}.

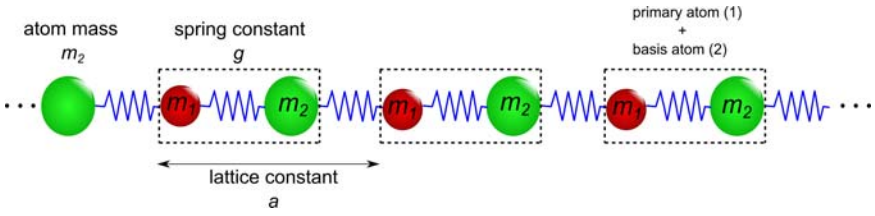

Fig. 1.17 Schematic of a 1D atomic chain with a two-atom basis.

In comparison to the monatomic chain, the index accounting for different atoms is more difficult when a basis atom is added (as well as any additional displacement dimensions not considered here); consequently, a matrix-based approach is required. To account for the discreteness of the

system, we represent each atom's displacement as $u_{n,\alpha}$ where α is the basis index (1 or 2) and n is the unit cell index. The equation of motion becomes (Ziman, 1972):

$$m_\alpha \ddot{u}_{n,\alpha} = -\sum_{m,\beta} \frac{\partial^2 U^{\text{harm}}}{\partial u_{n,\alpha} \partial u_{m,\beta}} u_{m,\beta} = -\sum_{m,\beta} \Phi_{n,\alpha}^{m,\beta} u_{m,\beta}, \tag{1.43}$$

where U^{harm} for this 2-atom basis is:

$$U^{\text{harm}} = \frac{1}{2} g \sum_n (u_{n,1} - u_{n,2})^2 + (u_{n,2} - u_{n+1,1})^2. \tag{1.44}$$

The matrix $\Phi_{n,\alpha}^{m,\beta}$ (hereafter called the 'force constants matrix') contains the interatomic force constants between each atom pair (i.e., (n,α) and (m,β)). Inspection of Eqs. (1.43) and (1.44) reveals:

$$\begin{aligned} \Phi_{n,1}^{n,1} = \Phi_{n,2}^{n,2} = 2g \\ \Phi_{n,2}^{n,1} = \Phi_{n,1}^{n,2} = \Phi_{n,1}^{n-1,2} = \Phi_{n,2}^{n+1,1} = -g. \end{aligned} \tag{1.45}$$

Recognizing the symmetry of the problem (i.e., that all unit cells are identical) and using a left-to-right numbering scheme, the force constants matrix becomes:

$$\Phi = \begin{bmatrix} 2g & -g \\ -g & 2g \end{bmatrix}. \tag{1.46}$$

From the translational symmetry of the chain, the unit cell indices n and m can be replaced by 0 and p, respectively, where p is simply an index that begins at 0 and increases in unit steps away from the cell of interest (i.e., 0). The Fourier transform of this matrix becomes the so-called dynamical matrix of lattice dynamics analysis (Young and Maris, 1989):

$$\begin{aligned} D_\alpha^\beta &= \frac{1}{\sqrt{m_\alpha m_\beta}} \Phi_{0,\alpha}^{p,\beta} e^{i\vec{K}\cdot\vec{r}_p} \\ &= \begin{pmatrix} \frac{2g}{m_1} & \frac{-g}{\sqrt{m_1 m_2}} \left(1 + e^{-iKa}\right) \\ \frac{-g}{\sqrt{m_1 m_2}} \left(1 + e^{+iKa}\right) & \frac{2g}{m_2} \end{pmatrix}, \end{aligned} \tag{1.47}$$

where $\vec{r}_p$ is the distance between the unit cells of the pair of atoms under consideration and implied summation applies to the index p. The dynamical

matrix emerges as part of the governing equation of motion (Eq. (1.43)) cast in frequency space:

$$\omega^2 \tilde{u}_\alpha(K) = \frac{1}{\sqrt{m_\alpha m_\beta}} \Phi_{0\alpha i}^{p\beta j} e^{iK\cdot\vec{r}_p} \tilde{u}_\beta(K) = D_\alpha^\beta \tilde{u}_\beta(K), \tag{1.48}$$

where $\tilde{u}$ is the amplitude of displacement. The so-called secular equation emerges from the foregoing expression and is used the extract the eigenvalues ω^2:

$$\det\left|\mathbf{D} - \omega^2 \mathbf{I}\right| = 0, \tag{1.49}$$

where $\mathbf{I}$ is the identity matrix (2 by 2 in this case). The solution of Eq. (1.49) provides a form of the dispersion relation:

$$\omega^4 - 2g\left(\frac{1}{m_1} + \frac{1}{m_2}\right)\omega^2 + \frac{4g^2}{m_1 m_2}\sin^2\left(\frac{Ka}{2}\right) = 0. \tag{1.50}$$

Using quadratic reduction, the foregoing result can be solved for ω^2:

$$\omega(K)^2 = g\left(\frac{1}{m_1} + \frac{1}{m_2}\right) \pm g\sqrt{\left(\frac{1}{m_1} + \frac{1}{m_2}\right)^2 - \frac{4}{m_1 m_2}\sin^2\left(\frac{Ka}{2}\right)}. \tag{1.51}$$

The '$\pm$' term in Eq. (1.51) produces the peculiarity of having two possible branches. The lower branch (defined as having the lower frequency, represented by ω_-) is the acoustic branch and is equivalent to that derived for the monatomic chain (Eq. (1.22)). The upper branch (ω_+), called the *optical branch*, is new and represents generally out-of-phase vibrations between neighboring atoms (i.e., the displacements of neighboring atoms are nearly equal and opposite). The limiting forms at the Brillouin zone origin and edges for both branches are:

$$\lim_{K\to 0} \omega_-(K) = Ka\sqrt{\frac{g\mu}{2m_1 m_2}}\,; \quad \lim_{K\to 0} \omega_+(K) = \sqrt{\frac{2g}{\mu}}, \tag{1.52}$$

$$\omega_-\left(K = \frac{\pi}{a}\right) = \sqrt{\frac{2g}{m_2}}\,; \quad \omega_+\left(K = \frac{\pi}{a}\right) = \sqrt{\frac{2g}{m_1}}, \tag{1.53}$$

where $\mu = (1/m_1 + 1/m_2)^{-1}$, and m_2 is the heavier of the two masses.

The two branches of the dispersion are shown in Fig. 1.18. The curves reveal an energy band gap between the branches that grows with increasing contrast between the two atomic masses. Moreover, the shape of the optical branch takes a generally flat character, suggesting that the group velocity $(d\omega/dK)$ is relatively small. Consequently, optical phonons are often neglected in the calculation of thermal conductivity, in favor of the acoustic branch.

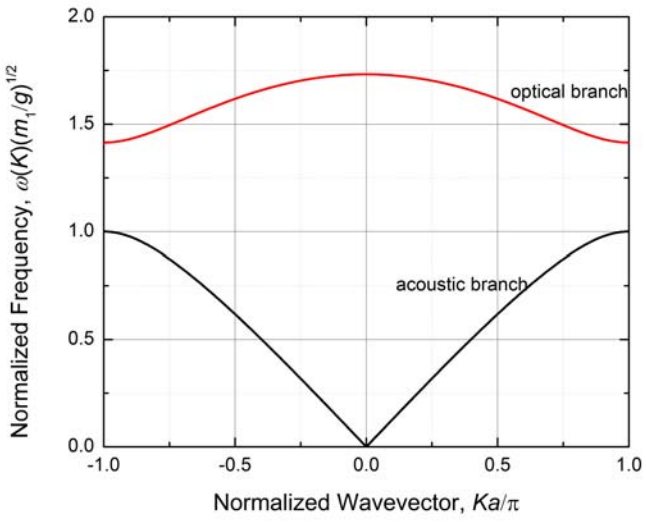

Fig. 1.18 Normalized frequency as a function of normalized wavevector for a diatomic 1D chain with $m_2 = 2m_1$.

Finally, we address a common source of confusion related to the application of the diatomic dispersion results to the case of $m_1 = m_2$ (i.e., the monatomic case). Figure 1.19 shows the dispersion curve for the range $K \in \{-\pi/a, \pi/a\}$. Notably, the solution still predicts the presence of an optical mode, and thus one might wonder whether the optical mode is simply an artifact of mathematics. However, careful inspection reveals that the condition $m_1 = m_2$ produces one-eighth of a full sine wave for the acoustic branch in the range $K \in \{0, \pi/a\}$ instead of the usual quarter sine wave (cf., Figs. 1.13 and 1.18). The reason for this change is that the diatomic analysis uses a lattice constant $a = 2\tilde{a}$ that is exactly twice as large as that

for the monatomic case ($a = \tilde{a}$) for this special case of $m_1 = m_2$. Therefore, the range of K sampled in Fig. 1.19 is only half that of Fig. 1.13. The missing portion of the dispersion curve is actually contained in the optical branch, as shown in Fig. 1.19, which spans $K \in \{0, 2\pi/a\}$ and shows the completion of the quarter sine wave by the 'virtual' optical branch. This result provides an example of the importance of defining the primitive unit cell, from which the 1st Brillouin zone derives, as the *smallest* symmetric region necessary to fill exactly all space through the translation vector $\vec{R}$.

1.7 Conclusion

This chapter has laid a foundation in crystallography and the fundamentals of phonons and electrons, albeit in a highly idealized and simplified form. Often the mathematics of these fundamentals can obscure more intuitive or at least more familiar understanding. For example:

- The speed of sound in silicon (Si) is approximately 6400 m/s. With its nearest neighbor distance of 0.235 nm and atomic mass of 28.0855 g/mol, it is a straightforward exercise to estimate the spring constant from the $K \to 0$ limit (Eq. (1.25)) as $g = 35$ N/m, which is remarkably similar to the actual value (Zhang *et al.*, 2007).
- Many metals have Fermi energies near $E_F = 5$ eV. The corresponding Fermi velocity is $v_F = \sqrt{2E_F/m_e} \approx 10^6$ m/s, which is roughly two orders of magnitude less than the speed of light, $c_0 = 2.99792458 \times 10^8$ m/s.

Lastly, we include here a brief glossary of some the concepts covered in this chapter:

- **Primitive Cell:** A region of space that is closer to one point than any others.
- **Bravais Lattice:** A distribution of points in space that defines a repeating pattern.
- **1st Brillouin Zone:** The primitive cell of the reciprocal lattice.
- **Miller Indices:** Coordinates (hkl) of the shortest reciprocal lattice vector normal to a given real-space plane.
- **Group Velocity:** The speed at which phonons carry energy in a lattice (see Eq. (1.24)).

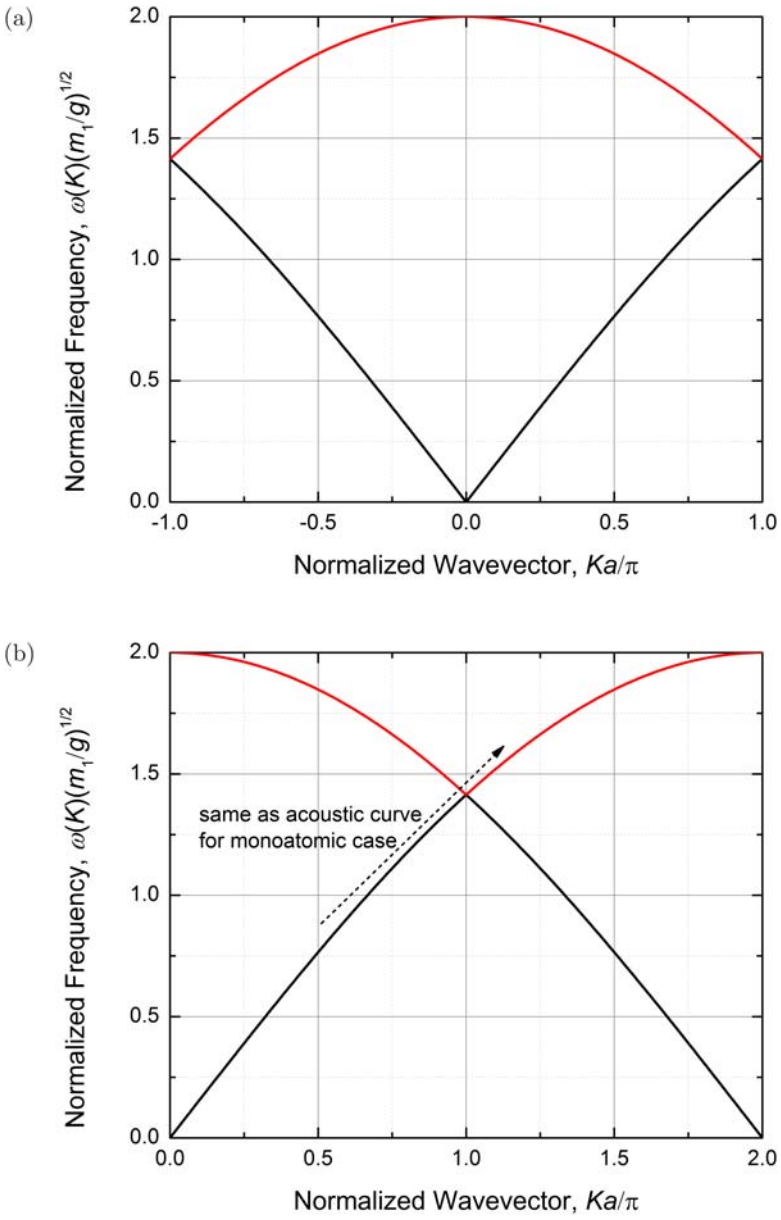

Fig. 1.19 Normalized frequency as a function of normalized wavevector for a diatomic 1D chain, for the special case of $m_1 = m_2$. (a) The usual range $K \in \{-\pi/a, \pi/a\}$. (b) The range $K \in \{0, 2\pi/a\}$.

- **Normal Mode:** A lattice wave that is characterized by a branch, wavevector, and frequency (and, later, polarization).
- **Phonon:** a quantized lattice vibration (i.e., one that can take on only a discrete energy, $\hbar\omega$).
- **Acoustic Phonons:** Phonons that determine the speed of sound in a solid and are characterized by $\omega \sim K$ as $K \to 0$.
- **Optical Phonons:** Phonons that have flat dispersion, low group velocity, and are characterized by non-zero ω as $K \to 0$.
- **Occupation Number:** The number of carriers with a given wavevector.

Example Problems

Problem 1.1: Graphene reciprocal lattice

The primitive lattice vectors ($\vec{a}_1$, $\vec{a}_2$) of graphene are given by:

$$\vec{a}_1 = \frac{3}{2}\tilde{a}\hat{x} + \frac{\sqrt{3}}{2}\tilde{a}\hat{y},$$

$$\vec{a}_2 = \frac{3}{2}\tilde{a}\hat{x} - \frac{\sqrt{3}}{2}\tilde{a}\hat{y},$$

where $\tilde{a}$ is the C-C bond length. Calculate the reciprocal lattice vectors $\vec{b}_1$, $\vec{b}_2$ of graphene. Show that the primitive unit cell of the reciprocal lattice (also known as the 1st Brillouin zone) is a hexagon with a side length of $\frac{4\pi}{3\sqrt{3}\tilde{a}}$.

Solution

The primitive lattice vectors are:

$$\vec{a}_1 = \frac{3}{2}\tilde{a}\hat{x} + \frac{\sqrt{3}}{2}\tilde{a}\hat{y}, \quad \vec{a}_2 = \frac{3}{2}\tilde{a}\hat{x} - \frac{\sqrt{3}}{2}\tilde{a}\hat{y}, \quad \vec{a_3} = c\hat{z}, \tag{1.54}$$

where c is an arbitrarily large constant (no periodicity exists in the z direction). The reciprocal lattice vectors are then given by:

$$\vec{b}_1 = 2\pi\frac{\vec{a}_2 \times \vec{a}_3}{\vec{a}_1 \cdot (\vec{a}_2 \times \vec{a}_3)}$$

$$= \frac{2\pi}{\tilde{a}}\left(\frac{1}{3}\hat{x} + \frac{1}{\sqrt{3}}\hat{y}\right), \tag{1.55}$$

$$\vec{b}_2 = 2\pi\frac{\vec{a}_3 \times \vec{a}_1}{\vec{a}_1 \cdot (\vec{a}_2 \times \vec{a}_3)}$$

$$= \frac{2\pi}{\tilde{a}}\left(\frac{1}{3}\hat{x} - \frac{1}{\sqrt{3}}\hat{y}\right), \tag{1.56}$$

$$\vec{b}_3 = 2\pi\frac{\vec{a}_1 \times \vec{a}_2}{\vec{a}_1 \cdot (\vec{a}_2 \times \vec{a}_3)}$$

$$= \frac{2\pi}{c}\hat{z}, \tag{1.57}$$

where $\vec{b}_3 \to 0$ as $c \to \infty$ indicating that the reciprocal lattice is two-dimensional. Figure 1.20 shows the process involved in construction of the reciprocal lattice. The Γ point of the reciprocal lattice is joined to its six nearest neighbors given by the points $\vec{b}_1$ (point A), $\vec{b}_2$ (point C), $\vec{b}_1 + \vec{b}_2$ (point B), $-\vec{b}_1$ (point D), $-\vec{b}_2$ (point F) and $-\vec{b}_1 - \vec{b}_2$ (point E). Perpendicular bisectors (red dotted lines in Fig. 1.20) are then drawn for each of these six line segments ΓA, ΓB, ΓC, ΓD, ΓE and ΓF. The region of intersection of these perpendicular bisectors forms the hexagonal Brillouin zone of graphene.

The side of the hexagon can be obtained from simple trigonometry. $\angle$MΓK $= \frac{1}{2}\angle$MΓB $= 30°$. Thus MK $=$ ΓM$/\sqrt{3} = |\vec{b}_1|/2\sqrt{3} = 2\pi/3\sqrt{3}\tilde{a}$. One side of the hexagonal Brillouin zone is 2MK $= 4\pi/3\sqrt{3}\tilde{a}$.

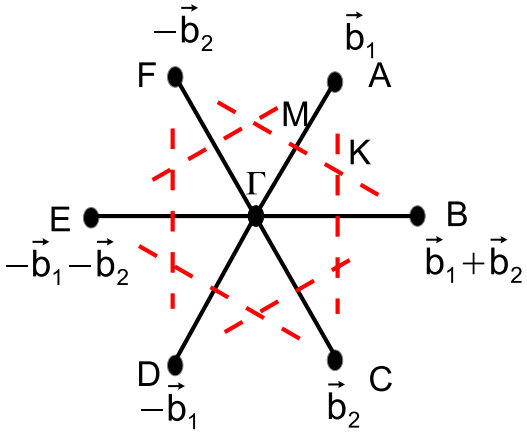

Fig. 1.20 Construction of the graphene Brillouin zone.

Problem 1.2: Dispersion relation for a 1D chain

(a) Consider a monoatomic 1D chain with nearest neighbor interactions. Assume a spring constant $g = 25$ N/m, atomic mass $m = 28$ amu and a lattice spacing of 5 Å. Calculate the sound velocity and the maximum possible phonon frequency.

(b) Now we generalize the monoatomic chain to include long-range interactions among atoms. Assume that the spring constant between two atoms separated by a distance of ja is given by g_j where j is an index that can take values $1, 2, 3$ and so on. Show that the new dispersion relation is given by:

$$\omega = 2\sqrt{\sum_j \frac{g_j \sin^2(\frac{1}{2}jKa)}{m}}.$$

Solution

(a) Sound velocity is given by:

$$c = a\sqrt{\frac{g}{m}} = 11594 \text{ m/s}, \tag{1.58}$$

where mass is converted to kg (1 amu $= 1.6605 \times 10^{-27}$ kg). The maximum phonon frequency is given by:

$$\omega_{\max} = 2\sqrt{\frac{g}{m}} = 4.63 \times 10^{13} \text{ rad/s}, \tag{1.59}$$

(b) When interactions are considered between all pairs of atoms, the equation of motion for the atom at position na is given by:

$$\begin{aligned} m\frac{d^2u(na)}{dt^2} &= \sum_{j=1}^{j=\infty} g_j(u[(n+j)a] - u(na)) - g_j(u(na) - u[(n-j)a]) \\ &= \sum_{j=1}^{j=\infty} g_j(u[(n+j)a] - 2u(na) + u[(n-j)a]). \end{aligned} \tag{1.60}$$

Substituting the plane wave solution $u(na) = \exp(i(Kna - \omega t))$ into the above equation produces:

$$-m\omega^2 = \sum_{j=1}^{j=\infty} g_j(\exp(ijKa) - 2 + \exp(-ijKa))$$

$$= \sum_{j=1}^{j=\infty} -4g_j \sin^2\left(\frac{jKa}{2}\right). \tag{1.61}$$

Thus the generalized dispersion relation is given by:

$$\omega = 2\sqrt{\sum_{j=1}^{j=\infty} \frac{g_j \sin^2(\frac{1}{2}jKa)}{m}}. \tag{1.62}$$

Problem 1.3: Kinetic energy of the free electron gas

Obtain an expression for the total kinetic energy of the free electron gas at $T = 0$ K. Express your answer in terms of the Fermi energy E_F and the total number of electrons N.

Solution

The following expressions for Fermi wavevector and Fermi energy were derived in the chapter:

$$k_F = (3\pi^2\eta_e)^{1/3}, \quad E_F = \frac{\hbar^2 k_F^2}{2m_e} = \frac{\hbar^2}{2m_e}(3\pi^2\eta_e)^{2/3}. \tag{1.63}$$

The volume of a spherical shell in $\mathbf{k}$-space with radius k and thickness dk is given by $4\pi k^2 dk$. The number of states in this shell is given by:

$$dN = 2\frac{4\pi k^2 dk}{(2\pi/L)^3}, \tag{1.64}$$

where the factor 2 accounts for spin degeneracy. The energy of each state on the spherical shell of radius k is $\hbar^2 k^2/2m_e$. The total energy of electrons is obtained by integrating up to the maximum wavevector k_F.

$$
\begin{aligned}
E &= \int_0^{k_F} \left(\frac{\hbar^2 k^2}{2m_e}\right)\left(2\frac{4\pi k^2 dk}{(2\pi/L)^3}\right) \\
&= \frac{\hbar^2 L^3}{2m_e\pi^2}\int_0^{k_F} k^4 dk \\
&= \frac{\hbar^2 L^3 k_F^5}{10 m_e \pi^2} \\
&= \frac{3}{5}\underbrace{\left(\frac{k_F^3 L^3}{3\pi^2}\right)}_{N}\underbrace{\left(\frac{\hbar^2 k_F^2}{2m_e}\right)}_{E_F} \\
&= \frac{3}{5} N E_F. \qquad (1.65)
\end{aligned}
$$

Problem 1.4: Phonon bandgap in a diatomic chain

Consider the diatomic chain (discussed in Section 1.6) with atomic masses m_1 and m_2. Assume that the spring constant is g for all the bonds. At what point in the Brillouin zone is the bandgap (difference between the optical and acoustic branch frequencies) a minimum? Obtain an expression for the non-dimensional bandgap (normalized by $\sqrt{g/m_1}$) as a function of the mass ratio m_2/m_1. Use the online Chapter 1 CDF tool[2] to observe the changes in shape of the acoustic and optical branches for varying mass ratio.

Solution

Observation of the acoustic and optical branches of a diatomic chain reveals that the bandgap is minimum at the edge of the Brillouin zone. The dispersion relation for a 1D diatomic chain of atoms is given by (see Eq. (1.51)):

$$
\omega(K)^2 = g\left(\frac{1}{m_1}+\frac{1}{m_2}\right) \pm g\sqrt{\left(\frac{1}{m_1}+\frac{1}{m_2}\right)^2 - \frac{4}{m_1 m_2}\sin^2\left(\frac{Ka}{2}\right)}. \qquad (1.66)
$$

[2] See http://nanohub.org/groups/cdf_tools_thermal_energy_course/wiki

The angular frequency at the edge of the Brillouin zone is obtained by substituting $K = \pi/a$:

$$\omega_-\left(K = \frac{\pi}{a}\right) = \sqrt{\frac{2g}{m_2}}, \quad \omega_+\left(K = \frac{\pi}{a}\right) = \sqrt{\frac{2g}{m_1}}. \tag{1.67}$$

The non-dimensional bandgap is given by:

$$\frac{\omega_+\left(K = \frac{\pi}{a}\right) - \omega_-\left(K = \frac{\pi}{a}\right)}{\sqrt{\frac{g}{m_1}}} = \sqrt{2}\left(1 - \sqrt{\frac{m_1}{m_2}}\right), \quad (m_2 > m_1). \tag{1.68}$$

From the above expression, the bandgap increases with increasing mismatch between the masses m_1 and m_2. Figure 1.21 shows snapshots of the dispersion curves from the online Chapter 1 CDF tool. The optical branch flattens and the maximum frequency of the acoustic branch reduces for increasing m_2/m_1.

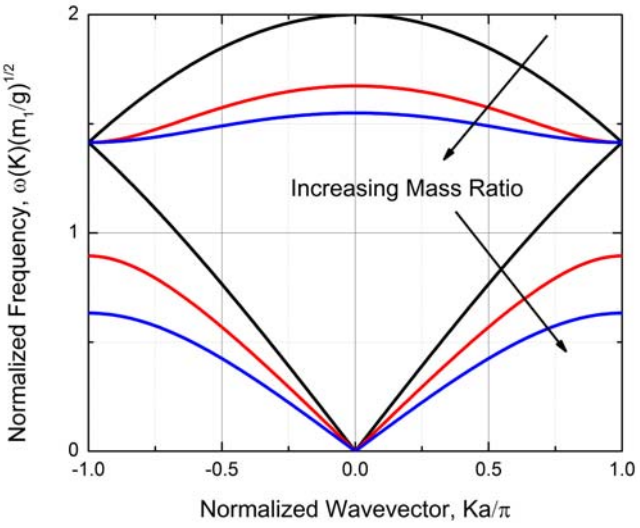

Fig. 1.21 Dispersion curves of the diatomic chain for increasing m_2/m_1.